Molecular Biology of the Cell
Vol. 12, 971–980, April 2001

Cell Cycle-Dependent Changes in Microtubule Dynamics in Living Cells Expressing Green Fluorescent Protein-α Tubulin[V]

Nasser M. Rusan, Carey J. Fagerstrom, Anne-Marie C. Yvon, and Patricia Wadsworth*

Department of Biology and Program in Molecular and Cellular Biology, University of Massachusetts, Amherst, Massachusetts 01003

Submitted August 23, 2000; Revised January 8, 2001; Accepted January 24, 2001
Monitoring Editor: Ted Salmon

LLCPK-1 cells were transfected with a green fluorescent protein (GFP)-α tubulin construct and a cell line permanently expressing GFP-α tubulin was established (LLCPK-1α). The mitotic index and doubling time for LLCPK-1α were not significantly different from parental cells. Quantitative immunoblotting showed that 17% of the tubulin in LLCPK-1α cells was GFP-tubulin; the level of unlabeled tubulin was reduced to 82% of that in parental cells. The parameters of microtubule dynamic instability were compared for interphase LLCPK-1α and parental cells injected with rhodamine-labeled tubulin. Dynamic instability was very similar in the two cases, demonstrating that LLCPK-1α cells are a useful tool for analysis of microtubule dynamics throughout the cell cycle. Comparison of astral microtubule behavior in mitosis with microtubule behavior in interphase demonstrated that the frequency of catastrophe increased twofold and that the frequency of rescue decreased nearly fourfold in mitotic compared with interphase cells. The percentage of time that microtubules spent in an attenuated state, or pause, was also dramatically reduced, from 73.5% in interphase to 11.4% in mitosis. The rates of microtubule elongation and rapid shortening were not changed; overall dynamicity increased 3.6-fold in mitosis. Microtubule release from the centrosome and a subset of differentially stable astral microtubules were also observed. The results provide the first quantitative measurements of mitotic microtubule dynamics in mammalian cells.

INTRODUCTION

Important advances in our understanding of the cytoskeleton have been made by direct observations of living cells following microinjection with fluorescent derivatives of cytoskeletal proteins (Desai and Mitchison, 1997). More recently, however, the ability to express cloned proteins containing a green fluorescent protein (GFP) tag has become the method of choice for dynamic analysis of the cytoskeleton (Chalfie *et al.*, 1994). GFP technology offers several significant advantages over the previous technology: it is not necessary to microinject cells, nor is it necessary to biochemically purify and fluorescently modify the protein of interest. However, there are also limitations to GFP technology: addition of GFP (238 amino acids) to the C or N terminus of the target protein can potentially interfere with protein function. In this regard, it is important to demonstrate that the chimeric protein retains its normal characteristics. In addition, overexpression of any protein can potentially interfere with cellular functions. This latter limitation can be overcome by the use of inducible promoters in the plasmid construct or by establishing permanent cell lines with the desired level of expression of the chimera.

To date, the dynamics of several cytoskeletal proteins have been examined using GFP technology. For example, transformation of yeast with a GFP-actin construct was used to document the motion of cortical actin patches (Doyle and Botstein, 1996). Although the GFP-actin did incorporate into dynamic actin-containing structures in the cells, the construct was not able to complement an actin null mutant (Doyle and Botstein, 1996). The major yeast tubulin gene *tub1* has also been tagged with GFP and this construct rescues a *tub1* mutant (Straight *et al.*, 1997). Importantly, observation of mitosis in yeast transformed with GFP-*tub1* provides strong evidence that spindle microtubules can undergo normal dynamic behavior in the expressing cells (Straight *et al.*, 1997). In other experiments, a fusion of GFP to the amino terminus of Tub1p did not complement a *tub1*

[V] Online version of this article contains video material and is available at www.molbiocell.org.

* Corresponding author. E-mail address: patw@bio.umass.edu.

deletion mutation, but yeast cells expressing a mixture of GFP-tagged and wild-type tubulin grew at normal rates (Maddox *et al.*, 1999). The dynamic behavior of individual microtubules has also been examined in yeast expressing an amino terminal fusion of GFP to a different yeast tubulin gene, *tub3*. The results show that yeast microtubules undergo dynamic instability behavior that is cell cycle regulated (Carminati and Stearns, 1997; Tirnauer *et al.*, 1999). In these experiments, addition of GFP to the amino terminus of *tub3*, but not to the carboxy terminus, was able to complement a *tub3* null mutation. Thus, the available data strongly support the view that expression of GFP-tubulin and its incorporation into microtubules does not detectably interfere with microtubule functions in yeast, and is therefore a valuable probe for analysis of microtubule behavior.

Heretofore, it has been extremely difficult to directly measure microtubule dynamics in mammalian cells throughout the cell cycle because of the difficulty of coordinating microinjection of fluorescent tubulin with the cell cycle and the fact that mitotic cells represent only a small fraction of the cells in a population. Other methods to visualize individual microtubules, such as differential interference contrast microscopy, are also more difficult in mitotic cells given their generally rounded morphology (Hayden *et al.*, 1990). Cells expressing GFP-tubulin have the potential to be an invaluable tool for studying microtubule dynamics, organization, and behavior throughout the cell cycle. To date, transient expression of GFP-tagged mouse β6-tubulin in cultured cells strongly suggests that microtubule dynamic behavior is not altered by expression of the GFP construct, although quantitative analysis of microtubule dynamics in these cells was not performed (Ludin and Matus, 1998; Heidemann *et al.*, 1999). In this work, we demonstrate that a cell line permanently expressing GFP-tubulin can be prepared and that the dynamic behavior of interphase microtubules in these cells is very similar to that in parental cells injected with rhodamine-labeled tubulin. We have used these cells to directly measure the changes in microtubule behavior throughout the cell cycle. In contrast to previous results in *Xenopus* egg extracts (Belmont *et al.*, 1990; Verde *et al.*, 1992; Tournebize *et al.*, 2000), our results demonstrate that both the frequency of catastrophe and of rescue are altered in mitotic compared with interphase cells. The percentage of time microtubules spend in an attenuated state, or paused, is also dramatically reduced in mitotic cells. The rates of elongation and rapid shortening are not changed. In addition to quantification of microtubule dynamic instability in mitotic cells, we document microtubule release from the centrosome and microtubule tethering at the cell cortex. The availability of cells expressing GFP-tubulin should provide a simple, easily manipulated system to examine microtubule behavior in mammalian cells.

MATERIALS AND METHODS

Materials

All materials for cell culture were obtained from Life Technologies (Gaithersburg, MD), with the exception of fetal calf serum, which was obtained from Atlanta Biologicals (Norcross, GA). Unless otherwise noted, all other chemicals were obtained from Sigma (St. Louis, MO).

Cell Culture and Cell Growth Assays

PtK_2 and LLCPK-1α cells were cultured in minimum essential medium supplemented with 1 mM sodium pyruvate, 10% fetal calf serum, and antibiotics, in an atmosphere of 5% CO_2, at 37°C. For observation, cells were plated on etched coverslips (Bellco Glass, Vineland, NJ) 1–2 d before use. To determine the mitotic index, cells were plated on coverslips, fixed in methanol, and stained with anti-tubulin antibodies (DM1-a; Sigma) and propidium iodide (0.5 μm); cells in prometaphase through late anaphase were counted from randomly selected fields; at least 200 cells were counted for each experiment. To determine the proliferation time, cells were plated in multiwell plates at low density and allowed to grow for 1 to 2 d before an initial cell count was made; subsequent counts of triplicate wells were made at various intervals following the initial count.

Microinjection

Cells were microinjected with fluorescent tubulin exactly as described previously (Yvon and Wadsworth, 1997). For injection of plasmid DNA, microinjection was performed in either the cytoplasm or the nucleus (Wadsworth, 1998). Plasmid DNA was purified using a QIAfilter Plasmid Maxi kit (Qiagen, Valencia, CA), resuspended in deionized distilled water, and injected at a concentration of 250–750 μg/ml.

Immunoblotting

Cell extracts from parental and transfected cells were prepared by harvesting cells, washing in phosphate-buffered saline, and lysing the cells in a buffer consisting of: 0.5% NP-40 in 50 mM HEPES, pH 7.5 with Pefablock, aprotinin, and leupeptin protease inhibitors. The cell lysate was centrifuged at 14,000 rpm for 30 min, and the supernatant recovered, boiled in SDS sample buffer, and run on a 10% polyacrylamide gel. All gel solutions were according to the formulations of Laemmli (1970). The proteins were transfered to polyvinylidene difluoride membrane (Hybond-P; Amersham Pharmacia Biotech, Piscataway, NJ), by using a Mini-transblot electrophoretic transfer cell, blocked for 1 h in 5% nonfat dry milk, and stained using an antibody to tubulin (clone DM1a; Sigma) at a dilution of 1:2000 for 1 h at 37°C. The blot was washed with Tris-buffered saline-Tween (25 mM Tris, pH 7.6; 137 mM NaCl; 3 mM KCl; 0.01% Tween) and incubated with an alkaline phosphatase-labeled secondary antibody, diluted 1:10,000 for 1 h at room temperature, with agitation. The membrane was washed again, and incubated with ECF reagent (Amersham Pharmacia Biotech) and scanned using a Storm Phosphorimager (Molecular Dynamics, Sunnyvale, CA).

Low Light Level Microscopy and Image Acquisition

For analysis of microtubule dynamics in interphase cells, a Nikon Eclipse TE 300 inverted microscope equipped with a 100× 1.3 numerical aperture objective lens was used. Images were acquired using a Micromax interline transfer cooled charge-coupled device camera (Roper Scientific, Trenton, NJ) and Metamorph software (Universal Imaging, Brandywine, PA). Exposure to the epi-illumination was controlled by an electronic shutter (Ludl; Electrical Products, Hawthorne, NY), also driven by Metamorph. Standard filter cubes G-1B and B-2E/C were used for acquisition of the rhodamine and GFP signals, respectively. For imaging, cells grown on coverslips were placed in Rose chambers (Rose *et al.*, 1958) in non-CO_2 DMEM lacking indicator dye and containing 0.3 U/ml Oxyrase oxygen scavenging system (EC Oxyrase; Oxyrase, Mansfield, OH). Time-lapse sequences were collected at 2-s intervals using an exposure time of 0.3–0.7 s for 2 min. Under these imaging conditions, little or no photobleaching or photodamage was observed, even when the oxyrase was omitted from the media. However, oxyrase was routinely included as a precautionary measure to limit any photobleaching or photodamage that might occur. To examine mi-

crotubule behavior in mitotic cells, both wide field fluorescence microscopy, as just described, and confocal fluorescence microscopy, were used. Sequences acquired using wide field fluorescence microscopy were used for tracking microtubule ends because all these images were acquired at 2-s intervals and at 35–37°C. Confocal microscopy was performed using a CSU-10, disk-scanning, direct-view confocal scanning unit (Perkin Elmer-Cetus Scientific, Gaithersburg, MD) attached to the Nikon Eclipse between the side port and the camera. Alternatively, the CSU-10 was used with a Leica microscope equipped with a 100× objective lens, and an Orca 1 charge-coupled device camera (Hammamatsu, Hammamatsu City, Japan). Finally, some observations were made using a Bio-Rad 600 confocal scan head attached to a Nikon Optiphot; images were acquired with a 60× 1.3NA objective lens, with the pinhole set at 1/3 open; Kalman averages, or a single, slow scan, were collected.

Microtubule Tracking

The behavior of individual microtubules was determined by tracking the position of the microtubule end by using the "track points" function of Metamorph, linked to an Excel spreadsheet. A life history plot of each microtubule was generated using Excel, and phases of growth, shortening, and pause were determined by eye as previously described (Dhamodharan *et al.*, 1995). Only changes >0.5 μm were considered growth or shortening events. The duration, distance, and velocity of growth and shortening events were determined for the selected phases by using Excel. The frequency of catastrophe was determined by dividing the sum of the number of transitions from growth to shortening and pause to shortening by the sum of the duration of growth and pause. The frequency of rescue was determined by dividing the sum of the number of transitions from shortening to growth and from shortening to pause by the time spent shortening. Dynamicity was calculated by dividing the sum of the total length grown and shortened by the life span of the microtubule. For LLCPK-1α cells, all parameters were determined for each microtubule with the exception of the percentage of time in a phase, which was determined for the population of microtubules. For transiently transfected PtK_2 cells, all parameters were determined for each microtubule, with the exception of catastrophe and rescue frequencies and percentage of time in a phase, which were determined for the population of microtubules. Statistical analysis was performed using MINITAB for windows (release 12).

Transfection

For transfection, cells were plated on coverslips, allowed to grow to ~60% confluence, and transfected using Lipofectamine (Life Technologies), according to the manufacturer's specifications. The GFP-α-tubulin plasmid was obtained from Clontech (Palo Alto, CA). To generate stable cell lines, transfected cells were selected with geneticin (G418), and fluorescent colonies were isolated using cloning rings (Bellco Glass). For measurement of microtubule dynamics in transiently transfected PtK_2 cells, cells were observed 24–48 h following transfection. Cells with microtubule arrays that appeared morphologically normal, and did not contain bundles of microtubules or other fluorescent structures, were used for analysis of microtubule dynamics.

RESULTS

Characterization of LLCPK-1α Cells Permanently Expressing GFP-Tubulin

A major goal of the present experiments was to determine whether mammalian cell lines permanently expressing GFP-tubulin could be established. The availability of such cells would provide the opportunity to study microtubule dynamics without the need for microinjection or transfection, and would facilitate analysis of transient stages of the cell cycle and/or rapid screening for microtubule-active compounds. We produced an LLCPK-1 cell line permanently expressing GFP-tubulin, which we call LLCPK-1α, and characterized cell growth and individual microtubule dynamics in these cells. Measurement of the mitotic index showed that a similar percentage of mitotic cells was present in both the parental cells and in LLCPK-1α (3.6 $\pm$ 0.42 versus 2.6 $\pm$ 0.80, respectively; n = 3 for each group). Measurements of proliferation showed that growth of LLCPK-1α cells was similar to the nontransfected parental line, with a doubling time of 20 h ($\pm$ 1.2), compared with 18 h ($\pm$ 1.2) for parental cells (n = 3 for each group). The changes we observed in mitotic index and doubling time were not statistically significant and the interphase and mitotic arrays of microtubules in these cells appeared normal, as did overall cellular morphology (our unpublished results).

Immunoblotting with an antibody to α-tubulin was used to determine the level of expression of GFP-α tubulin in these cells. Extracts of LLCPK-1α cells showed two bands, one corresponding to α-tubulin and one to GFP-α tubulin. Quantification showed that the GFP-α tubulin represented 17% of the total α-tubulin in these cells. Interestingly, the level of untagged α-tubulin in the LLCPK-1α cells was reduced to 82% of the level in the parental line, demonstrating that the addition of GFP did not interfere with the autoregulation of α-tubulin level in these cells (Yen *et al.*, 1988).

Quantification of Interphase Microtubule Dynamics in LLCPK-1α Cells

To determine whether the presence of GFP-α tubulin altered microtubule behavior, the dynamics of individual interphase microtubules in LLCPK-1α cells and parental LLCPK-1 cells injected with rhodamine-labeled tubulin was measured and compared. Image sequences of the cell periphery, where individual microtubules were clearly observed, were acquired at 2-s intervals. Observation of interphase microtubules in both the injected parental (Figure 1A) and LLCPK-1α cells (Figure 1B) revealed that the microtubules were dynamic, alternating between phases of growth, shortening, and pause. In addition, a subpopulation of differentially stable microtubules was also observed (Shelden and Wadsworth, 1993). Stable microtubules, defined here as those that did not show any dynamic events during an image sequence (typically 2 min; see "Methods"), were more frequently observed in lamella extending away from a cell patch than in lamella contacting other cells in the patch, for both cells injected with rhodamine tubulin or expressing GFP tubulin (our unpublished results). The percentage of stable microtubules in a cell was highly variable for both rhodamine-tubulin injected and GFP-tubulin expressing cells. Given this cell-to-cell variability, quantitative measurements are reported for cells in which >50% of the trackable microtubules were dynamic, not stable. For each cell used in analysis, both the stable and dynamic microtubules were tracked and included in the reported results.

The parameters of dynamic instability were measured from life history plots of individual microtubules (Figure 1,

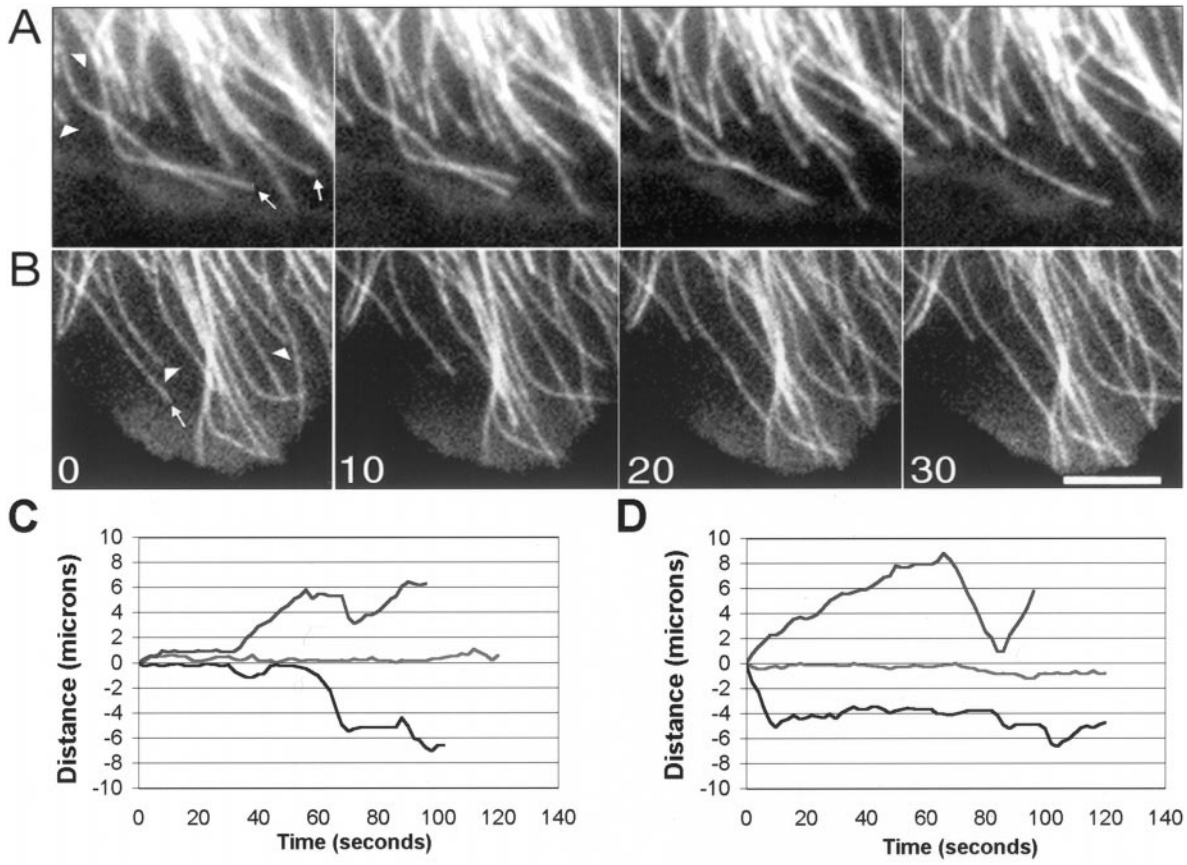

Figure 1. Image sequences of microtubule dynamic behavior in living LLCPK-1 cells injected with rhodamine tubulin (A) and in LLCPK-1α cells expressing GFP-tubulin (B). Images were collected at 2-s intervals and are shown at 10-s intervals. Arrows indicate shortening events; arrowheads indicate growth events. Bar, 5 μm. Life history plots showing the dynamic behavior of individual microtubules in LLCPK-1 cells injected with rhodamine tubulin (C) and LLCPK-1α cells expressing GFP-tubulin (D). The life history plots shown in C and D are from different cells than shown in A and B. Most microtubules in these cells displayed periods of growth, shortening, and pause (upper and lower traces in C and D); a subset of microtubules was differentially stable (middle traces, C and D). Only cells in which >50% of the trackable microtubules were dynamic were included in the data set; for all cells analyzed, all trackable microtubules in the cell were included in the analysis.

C and D). Comparison of the dynamic parameters showed that the behavior of GFP-containing microtubules was remarkably similar, but not identical, to the behavior of microtubules in cells injected with rhodamine-labeled tubulin (Table 1). The average distance, duration, and rate of growth excursions were not significantly different between the two groups. For shortening excursions, the distance and rate were not different, but the average duration of shortening excursions was increased by 18.2%. This difference was statistically significant. Other parameters of dynamics, including the frequencies of catastrophe and rescue and dynamicity, a measure of the total subunit addition and loss at microtubule plus-ends per minute, were not different between the two groups. The major difference between the GFP-tubulin containing and the rhodamine tubulin-injected cells was a 28.3% increase in the average duration of pause events in the GFP-tubulin–expressing cells.

Microtubule dynamics was also measured in PtK_2 cells either transiently transfected with GFP-tubulin (see "Methods") or injected with rhodamine-labeled tubulin. As observed with LLCPK-1α cells, microtubule dynamics was very similar, but not identical, in the two situations. The major difference between rhodamine tubulin– and GFP-tubulin–containing microtubules was a statistically significant increase in both the rates of growth and shortening (8.9 versus 10.2 μm/min, and 9.5 versus 12 for rhodamine tubulin- and GFP tubulin-containing microtubules, respectively). No significant differences in the average distance and duration of growth or shortening excursions or in the duration of pause events were detected. The frequencies of catastrophe and rescue were determined for the population of microtubules (see "Methods") and were found to be very similar (frequency of catastrophe: 0.019 versus 0.021 s^{-1} and frequency of rescue: 0.112 versus 0.109 s^{-1}, for rhodamine tubulin– and GFP-tubulin–containing microtubules, respectively). Transiently transfected PtK_2 cells were subsequently subjected to selection in G418, yielding a population of cells in which the majority express GFP-tubulin.

Table 1. Quantitation of MT dynamic behavior in rhodamine tubulin-injected interphase cells, and in EGFP-tubulin-expressing cells in interphase and mitosis

	Interphase cells		Mitotic cells
Dynamic Parameters	Rhodamine tubulin 42 MTs	EGFP tubulin 62 MTs	EGFP tubulin 28 MTs
Growth			
Rate (μm/min)	11.50 ± 7.14	11.50 ± 7.40	12.76 ± 5.66
Distance (μm)	1.10 ± 0.77	1.22 ± 0.93	3.14 ± 1.59[a]
Duration (s)	6.25 ± 3.69	7.20 ± 4.96	17.0 ± 12.2[a]
Shrink			
Rate (μm/min)	14.8 ± 8.54	13.1 ± 8.43	14.14 ± 7.86
Distance (μm)	1.37 ± 1.37	1.52 ± 1.77	3.70 ± 3.83[a]
Duration (s)	5.49 ± 3.41[a]	6.71 ± 4.28	13.22 ± 7.65[a]
Average pause duration (s)	18.3 ± 25.7[b]	25.5 ± 32.7	9.31 ± 5.08[a]
% Time per phase (growth/shrink/pause)	16.7/12.8/70.5	15/11.5/73.5	50.5/38.1/11.4
Rescue frequency (s^{-1})	0.203 ± 0.092	0.175 ± 0.104	0.045 ± 0.111[a]
Catastrophe frequency (s^{-1})	0.035 ± 0.024	0.026 ± 0.024	0.058 ± 0.045[a]
Dynamicity (μm/min)	4.5 ± 2.8	4.0 ± 3.5	14.6 ± 11.3[a]

EGFP, enhanced green fluorescent protein; MT, microtubule.

[a] Significant from EGFP tubulin interphase cells at 99.9% confidence level.

[b] Significant from EGFP tubulin interphase cells at 95% confidence level.

All statistics analyzed using a Student's *t* test.

Quantification of Microtubule Dynamic Instability in Mitotic Cells

Given the similarity of microtubule dynamic behavior in parental and LLCPK-1α cells in interphase, we used these cells to observe and quantify microtubule behavior in mitotic cells. For these experiments, cells in late prometaphase or metaphase were selected and images were collected at 2-s intervals. At the end of the sequence, we verified that the cell had not progressed into anaphase. Individual astral microtubules extending toward the cell periphery, and not toward the chromosomes, were tracked from the image sequences (see "Methods").

Measurements of microtubule behavior showed that the mitotic microtubules were highly dynamic as observed previously in *Xenopus* extracts (Belmont *et al.*, 1990) (Figure 2A). The parameters of dynamic instability were determined from the life history plots (Figure 2B). The average rates of growth and shortening were not statistically significantly different in interphase and mitotic cells, but both the duration and distance of these events were greater in mitotic than interphase cells (Table 1). In addition, a dramatic decrease in the time spent in a state of attenuated dynamics, or pause, was noted. Specifically, microtubules in interphase cells spent 73.5% of the time in pause; this value was reduced to 11.4% in mitotic cells. The average pause duration was also reduced in mitotic cells, from 25.5 s in interphase to 9.3 s in mitosis; this difference was statistically significant.

Determination of the transition frequencies showed that both the frequency of rescue and of catastrophe were significantly different in mitotic compared with interphase cells. The frequency of rescue was decreased nearly fourfold from 0.175 to 0.045 s^{-1}. The frequency of catastrophe was increased twofold from 0.026 to 0.058 s^{-1}. Finally, the overall dynamicity of the microtubules was increased nearly fourfold, from 4.0 to 14.6 μm/min (Table 1). Movie sequences of microtubule behavior in mitotic cells can be viewed with the online version of this article.

During analysis of image sequences, we observed a small number of astral microtubules whose behavior was characterized by long periods of pause (Figure 3). In some sequences, a microtubule was paused at the cell cortex and subsequently disassembled; in other cases we observed the microtubule grow out to the cortex and then pause (Figure 3). Less frequently we observed a microtubule that paused for the entire image sequence. In all cases, the paused microtubules were well separated from the majority of dynamic microtubules near the aster center and appeared to terminate at the cell periphery. The dynamic parameters of the differentially stable astral microtubules were not included in the analysis reported in Table 1.

Release of Mitotic Microtubules

Observations of spindles and asters assembled in vitro have demonstrated that microtubules are released and translocated away from the centrosome with the plus-end leading (Belmont *et al.*, 1990); microtubule release has also been observed in interphase cells (Keating *et al.*, 1997). We examined movie sequences of living mitotic cells to determine whether microtubule release occurred in vivo. Figure 4 shows an example of a released microtubule that initially moves toward the cell cortex with little change in length, and subsequently shortens considerably from the minus-end (Figure 4). We also observed two instances in which a mi-

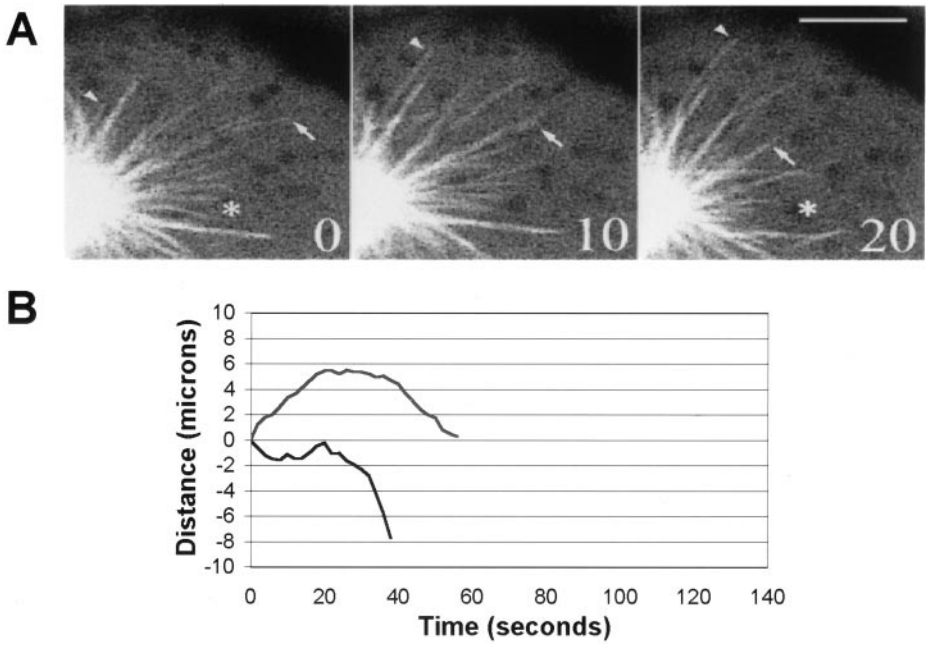

Figure 2. Microtubule behavior in mitotic cells. (A) Dynamic behavior of astral microtubules in LLCPK-1α cells; images shown were collected at 10-s intervals by using the Bio-Rad confocal microscope. The arrowhead shows a microtubule that grows out from the aster center; the arrow shows a shortening microtubule. The asterisk marks the same pixel location in the first and last images. Bar, 5 μm. (B) Life history plots of mitotic microtubles in LLCPK-1α cells. Each line on the graph represents the excursions made by an individual microtubule plus-end during the observation period. The majority of microtubules either grew out from the aster, followed by a catastrophe transition (upper trace), or were in the field of view at the start of the image sequence and subsequently underwent a catastrophe and disassembled out of the field of view (lower trace). The life history plots shown in B are from different cells than shown in A.

crotubule grew out to the cell cortex, paused, and subsequently began rapid shortening from the minus-end toward the stationary plus-end. Although release and shortening of a microtubule minus-end with the plus-end at the cell cortex was relatively rare, we more frequently observed small microtubule fragments at the cortex that may have resulted from release and incomplete disassembly of a microtubule with an attached plus-end.

Analysis of the behavior of released microtubules shows that, in some cases, the behavior of the ends was coordinated, as would be observed during transport or treadmilling. In most instances, however, the behavior of the two ends of the microtubule was different (Figure 4). Minus-ends of released microtubules (n = 10) spent 16.4% of the observation time in pause and the remaining 83.6% moved away from the centrosome. Consistent with previous observations in interphase cells, released minus-ends did not undergo growth (Keating *et al.*, 1997; Vorobjev *et al.*, 1997; Yvon and Wadsworth, 1997). Plus-ends of released microtubules (n = 9) spent 22.3% of the observation time in pause and the remaining 77.7% moved toward the cell cortex. The plus-ends of released microtubules were not observed to shorten, in contrast to the plus-ends of microtubules that were not released, which spent 38.1% of the time shortening (Table 1). This suggests that the dynamic behavior may have changed from dynamic instability to treadmilling (Rodionov *et al.*, 1999).

The rate of motion of plus- and minus-ends was measured. Assuming that motion of the plus-ends was due to subunit addition, the rate of growth at the plus-ends (15 μm/min) was similar to plus-end growth of nonreleased microtubules (Table 1) and to treadmilling in interphase cells (~12 μm/min) (Rodionov *et al.*, 1999). Assuming that motion at the minus-end was due to subunit loss, the average rate of shortening of the minus-ends (24 μm/min) was greater than both the rate of subunit loss during treadmilling (~12 μm/min) and minus-end shortening in interphase cells (~5 μm/min) (Vorobjev *et al.*, 1997; Waterman-Storer and Salmon, 1997; Yvon and Wadsworth, 1997; Rodionov *et al.*, 1999; Vorobjev *et al.*, 1999), suggesting that the rate of subunit loss from minus-ends may be regulated in mitosis. Although the behavior of released microtubules is consistent with subunit addition and loss from microtubule ends by dynamic instability and/or treadmilling, microtubule transport may also contribute to the observed motion. In support of this possibility, the rates of microtubule motion in mitotic cells are consistent with the rates of microtubule transport in interphase cells (9–40 μm/min) (Keating *et al.*, 1997).

Although release events were sometimes difficult to detect due to the high background fluorescence in these mitotic cells, we estimate that the frequency of release from the aster was 0.05 events/min (22 release events in 410 min of observation).

DISCUSSION

Characterization of LLCPK-1α Cells Expressing GFP-Tubulin

The results of our experiments demonstrate that the parameters of microtubule dynamics in interphase cells expressing GFP-tubulin were remarkably similar to dynamics in parental cells injected with rhodamine-labeled brain tubulin. From these data, we conclude that microtubule dynamics has not been extensively altered by the presence of the GFP tag on α tubulin, and that cells permanently expressing or transiently transfected with GFP-tubulin are a useful tool for the analysis of microtubule behavior in diverse cells. Although the presence of the GFP tag may contribute to the relatively minor alterations in dynamics that we observed, it should be noted that the intrinsic variability in microtubule behavior

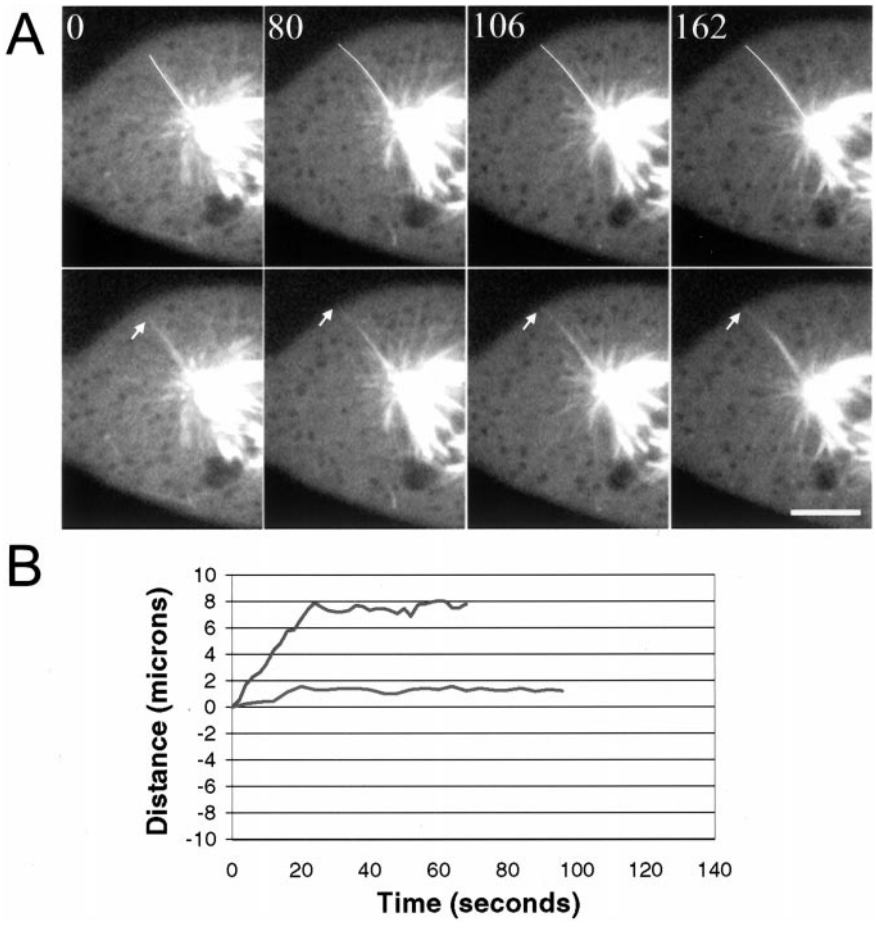

Figure 3. Differentially stabilized astral microtubules in mitotic cells. (A) Image sequence showing an astral microtubule that grows out to the cell edge and then pauses for the remainder of the sequence. The microtubule end is marked by the arrow. In the upper panels, the microtubule has been colored white to aid in visualization. Images were acquired using the Ultraview confocal microscope at 2-s intervals; Bar, 5 μm. (B) Life history plots of the dynamic behavior of individual stable, astral microtubules. The microtubule shown in the upper trace grew toward the cell cortex where it was relatively stable for the remainder of the movie sequence; the microtubule in the lower trace was inactive for the entire sequence. The life history plots shown in B are from different cells than shown in A.

(Vorobjev *et al.*, 1997; Waterman-Storer and Salmon, 1997; Wadsworth, 1999) and/or limitations in measurement of microtubule dynamics (Shelden and Wadsworth, 1993) could also contribute to these differences.

Modulation of Transition Frequencies and Pause in Mitotic Cells

Our observations show that in mammalian somatic cells, the frequency of catastrophe is increased and the frequency of rescue is decreased when cells progress into mitosis. This is in contrast to the situation in *Xenopus* extracts, where the major difference in microtubule dynamics between mitotic and interphase extracts is an increase in the frequency of catastrophe (Table 2; Belmont *et al.*, 1990; Verde *et al.*, 1992; Tournebize *et al.*, 2000). Previous work has shown that rescue events are frequent in interphase mammalian cells, especially those of epithelial origin, and it was proposed that modulation of rescue frequency could be responsible for the change in microtubule dynamics from interphase to mitosis (Cassimeris *et al.*, 1988; Shelden and Wadsworth, 1993). Our results now demonstrate that in mammalian tissue culture cells the frequency of rescue is decreased as cells progress into mitosis, thus contributing to the regulation of microtubule dynamics throughout the cell cycle.

A second major change in microtubule dynamics in mitotic cells was the dramatic reduction in pause. Unlike microtubules in embryonic extracts, microtubles in interphase cells spend a considerable amount of time in a state of attenuated dynamics or pause (Shelden and Wadsworth, 1993). Our results demonstrate that, in addition to modulation of transition frequencies, pause is reduced when somatic cells progress into mitosis.

It is important to note the similarities and differences between our measurements in live cells and those in cell extracts. In live cells, individual microtubule behavior could not be resolved in the central spindle, so only astral microtubules were measured. This is consistent with the measurements made in *Xenopus* extracts, which measured microtubules nucleated from centrosomes (Belmont *et al.*, 1990; Verde *et al.*, 1992; Tournebize *et al.*, 2000). In extracts, the concentration of rhodamine-labeled tubulin in the extract was ~1 mg/ml, which is significantly greater than the level of GFP-tubulin or rhodamine tubulin used in live cell experiments. The level of rhodamine-labeled tubulin could affect the measurement of dynamics in extracts, as previously noted (Belmont *et al.*, 1990). Experiments in extracts are performed in a thin layer of cytoplasm, near the coverslip surface, which differs from the situation in living cells. Finally, in both types of experiment, microtubule dynamics

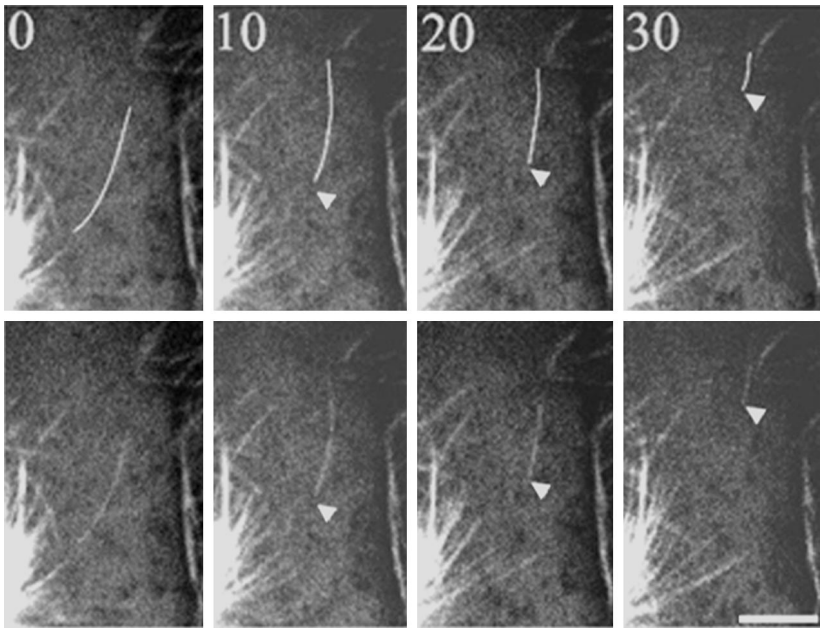

Figure 4. Astral microtubules are released from the centrosome in mitotic cells. In the upper panels the released microtubule has been colored white to aid in visualization. In this sequence, a microtubule is released and appears to move away from the aster center; the microtubule end was not clear before the image labeled t = 0. The minus-end most likely moved into the field of view by transport or disassembly following release; no evidence for a severing event was detected. Time is given in seconds in each frame. Bar, 5 μm.

was measured only in prometaphase and metaphase cells; additional changes in microtubule dynamics may occur as cells enter mitosis in prophase and exit mitosis in telophase.

Rates of Microtubule Growth and Shortening Do Not Change throughout the Mammalian Cell Cycle

Our results demonstrate that the rates of microtubule growth and shortening did not vary significantly throughout the mammalian cell cycle (Table 2). This result is in agreement with measurements in *Xenopus* extracts, which report that the rates of growth and shortening are similar throughout the cell cycle (Table 2; Belmont *et al.*, 1990; Verde *et al.*, 1992; Tournebize *et al.*, 2000). In newt lung cells, however, the rate of microtubule growth was twice as fast in mitotic compared with interphase cells (Table 2; Hayden *et al.*, 1990). In yeast, microtubule dynamics are more rapid in G1 than in mitosis, consistent with the view that dynamic microtubules are required to position the spindle in G1 before mitosis (Carminati and Stearns, 1997; Shaw *et al.*, 1997; Tirnauer *et al.*, 1999). The increase in dynamics is accomplished by changes in both transition frequencies and in the rates of growth and shortening (Table 2; Tirnauer *et al.*, 1999). Interestingly, recent experiments show that depletion of a major growth-promoting microtubule-associated protein, XMAP215, from *Xenopus* extracts reduced the velocity of microtubule growth in interphase, but not mitotic, extracts (Tournebize *et al.*, 2000), indicating that different regulatory factors are active at different times in the cell cycle. Thus, it is possible that the similar velocities of microtubule growth and shortening measured throughout the

Table 2. Comparison of microtubule dynamic parameters in interphase and mitosis

Dynamic Parameter	Mammalian[a]		*Xenopus*[b]		Newt lung cells		Yeast[c]	
	Interphase	Mitosis	Interphase	Mitosis	Interphase[d]	Mitosis[e]	Interphase	Mitosis
f_{cat}^{+}	0.026	0.058	0.018	0.12	0.014	nd	0.008	0.004
f_{res}^{+}	0.175	0.045	0.011	0.02	0.044	nd	0.007	0.002
V_{gr}^{++}	11.5	12.8	9.3	12.3	7.2	14.3	2.2	1.7
V_{sh}^{++}	13.1	14.1	12.8	15.3	17.3	~16	3.2	2.7

f_{cat}, frequency of catastrophe; f_{res}, frequency of rescue; V_{gr}, velocity of growth; V_{sh}, velocity of shortening.
+, sec^{-1}; ++, μm/min.

[a] This report.

[b] Belmont *et al.* (1990).

[c] Cassimeris *et al.* (1988).

[d] Hayden *et al.* (1990).

[e] Tirnauer *et al.* (1999).

mammalian cell cycle result from the activity of different combinations of regulatory factors.

Differential Stability of Astral Microtubules in Mammalian Cells

Our observations of astral microtubule dynamics in mitotic cells showed that a subset of microtubules is differentially stable, and that the plus-ends of these microtubules are often located near the cell edge, or cortex. Interactions between the ends of these microtubules and the cell cortex may contribute to spindle positioning (Busson *et al.*, 1998; O'Connell and Wang, 2000; Tirnauer and Bierer, 2000). For example, recent work has shown that the yeast protein Bim1p, a member of the EB1 protein family, localizes to microtubule plus-ends, modulates microtubule dynamics, and contributes to spindle positioning via interactions with the cortical protein Kar9p (Berrueta *et al.*, 1998; Morrison *et al.*, 1998; Korinek *et al.*, 2000; Lee *et al.*, 2000; Tirnauer and Bierer, 2000). Plus-end specific microtubule-associated proteins in mammalian cells are likely to contribute to the difference in dynamic behavior of the stable subset of microtubules and to mediate interactions of these microtubules with cortical molecules (Tirnauer and Bierer, 2000).

Microtubule Release from the Centrosome

Microtubule release from the centrosome has been observed in interphase and mitotic *Xenopus* extracts and in living interphase cells (Belmont *et al.*, 1990; Keating *et al.*, 1997; Vorobjev *et al.*, 1997; Waterman-Storer and Salmon, 1997; Waterman-Storer *et al.*, 2000). Marking experiments performed on released microtubules in interphase cells demonstrate that individual released microtubules can undergo treadmilling, transport, and minus-end disassembly (Keating *et al.*, 1997). Although we have not marked the microtubule lattice of the released microtubules, our observations are consistent with multiple mechanisms contributing to the movement of released microtubules in these cells. Our estimate of the rate of release, 0.05 events/min, was markedly slower than most, but not all, previous measurements. For example, release rates of 0.5, 0.02, and 3.6 releases/min have been reported for interphase mammalian and newt lung cells and *Xenopus* mitotic extracts, respectively (Belmont *et al.*, 1990; Vorobjev *et al.*, 1997; Waterman-Storer and Salmon, 1997). The high rate of release in extracts may be due, in part, to the adsorption of motors to the coverslip surface, although recent work demonstrates that changes in the integrity of astral arrays occur in solution as well as on the coverslip surface (Waterman-Storer *et al.*, 2000). Several factors could contribute to the lower rate of release in these mitotic cells. First, release may be regulated in a cell cycle-dependent manner. Second, we may have underestimated release due to the difficulty in detecting individual fluorescent microtubules in these somewhat rounded mitotic cells. Third, the rate of release may vary in different regions of mitotic cells; for example, release may occur more frequently in the central spindle (McDonald *et al.*, 1992; Mastronarde *et al.*, 1993). Additional measurements are necessary to resolve these issues.

Summary

Our results demonstrate that cell lines permanently expressing GFP-tubulin can be established and that the dynamic behavior of individual interphase microtubules in these cells is very similar to microtubule behavior in parental cells injected with rhodamine-labeled tubulin. Measurements of the behavior of astral microtubules in mitotic cells demonstrate that both the frequency of catastrophe and of rescue are modulated when cells enter mitosis; pause is also dramatically reduced in mitotic cells. Our results are consistent with the view that a highly regulated balance of the activity of different factors is responsible for regulation of microtubule dynamics throughout the cell cycle (Andersen, 1999). These GFP-expressing cells will be a useful tool to elucidate the regulation of microtubule dynamic turnover throughout the cell cycle.

ACKNOWLEDGMENTS

We are grateful to Jonathan Walker for assistance in the determination of the mitotic index, to Mia Sorcinelli for tracking microtubules, and to Dr. Mary Ann Jordan for advice concerning proliferation assays. We thank Dr. Joe Kunkel for invaluable assistance with Excel spreadsheets. We thank Dr. Shinya Inoué for allowing us to use the confocal microscope to record microtubule behavior in mitotic cells. We acknowledge Dr. Barbara Danowski for advice, encouragement, and for keeping us sane as we tracked microtubules. This work was supported by grants from the National Science Foundation and National Institutes of Health to P.W.

REFERENCES

Andersen, S.S.L. (1999). Balanced regulation of microtubule dynamics during the cell cycle: a contemporary view. BioEssays *21*, 53–60.

Belmont, L.D., Hyman, A.A., Sawin, K.E., and Mitchison, T.J. (1990). Real-time visualization of cell cycle dependent changes in microtubule dynamics in cytoplasmic extracts. Cell *62*, 579–589.

Berrueta, L., Kraeft, S.-K., Tirnauer, J.S., Schuyler, S.C., Chen, L.B., Hill, D.E., Pellman, D., and Bierer, B.E. (1998). The adenomatous polyposis coli-binding protein EB1 is associated with cytoplasmic and spindle microtubules. Proc. Natl. Acad. Sci. USA *95*, 10596–10601.

Busson, S., Dujardin, D., Moreau, A., Dompierre, J., and DeMay, J.R. (1998). Dynein and dynactin are localized to astral microtubules and at cortical sites in mitotic epithelial cells. Curr. Biol. *8*, 541–544.

Carminati, J., and Stearns, T. (1997). Microtubules orient the mitotic spindle in yeast through dynein-dependent interactions with the cell cortex. J. Cell Biol. *138*, 629–641.

Cassimeris, L.U., Pryer, N.K., and Salmon, E.D. (1988). Real-time observations of microtubule dynamic instability in living cells. J. Cell Biol. *107*, 2223–2231.

Chalfie, M., Tu, Y., Euskirchen, G., Ward, W.W., and Prasher, D.C. (1994). Green fluorescent protein as a marker for gene expression. Science *263*, 802–805.

Desai, A., and Mitchison, T. (1997). Microtubule polymerization dynamics. Annu. Rev. Cell Dev. Biol. *13*, 83–117.

Dhamodharan, R., Jordan, M.A., Thrower, D., Wilson, L., and Wadsworth, P. (1995). Vinblastine suppresses dynamics of individual microtubules in living interphase cells. Mol. Biol. Cell *6*, 1215–1229.

Doyle, T., and Botstein, D. (1996). Movement of yeast cortical actin cytoskeleton visualized *in vivo*. Proc. Natl. Acad. Sci. USA *93*, 3886–3891.

Hayden, J.H., Bowser, S.S., and Rieder, C.L. (1990). Kinetochores capture astral microtubules during chromosome attachment to the mitotic spindle: direct visualization in live newt lung cells. J. Cell Biol. *111*, 1039–1045.

Heidemann, S.R., Kaech, S., Buxbaum, R.E., and Matus, A. (1999). Direct observations of the mechanical behaviors of the cytoskeleton in living fibroblasts. J. Cell Biol. *145*, 109–122.

Keating, T.J., Peloquin, J.G., Rodionov, V.I., Momcilovic, D., and Borisy, G.G. (1997). Microtubule release from the centrosome. Proc. Natl. Acad. Sci. USA *94*, 5078–5083.

Korinek, W.S., Copeland, M.J., Chaudhuri, A., and Chant, J. (2000). Molecular linkage underlying microtubule orientation toward cortical sites in yeast. Science *287*, 2257–2259.

Laemmli, U.K. (1970). Cleavage of structural proteins during the assembly of the head of bacteriophase T4. Nature *227*, 680–685.

Lee, L., Tirnauer, J.S., Li, J., Schuyler, S.C., Liu, J.Y., and Pellman, D. (2000). Positioning of the mitotic spindle by a cortical microtubule capture mechanism. Science *287*, 2260–2262.

Ludin, B., and Matus, A. (1998). GFP illuminates the cytoskeleton. Trends Cell Biol. *8*, 72–77.

Maddox, P., Chin, E., Mallavarapu, A., Yeh, E., Salmon, E.D., and Bloom, K. (1999). Microtubule dynamics from mating through the first zygotic division in the budding yeast *Saccharomyces cerevisiae.* J. Cell Biol. *144*, 977–987.

Mastronarde, D.N., McDonald, K.L., Ding, R., and McIntosh, J.R. (1993). Interpolar spindle microtubules in PtK cells. J. Cell Biol. *123*, 1475–1489.

McDonald, K.L., O'Toole, E., Ding, R., and McIntosh, J.R. (1992). Kinetochore microtubules in PtK cells. J. Cell Biol. *118*, 369–383.

Morrison, E.E., Wardleworth, B.N., Askham, J.M., Markham, A.F., and Meredith, D.M. (1998). EB1, a protein which interacts with the APC tumor suppressor, is associated with the microtubule cytoskeleton throughout the cell cycle. Oncogene *17*, 3471–3477.

O'Connell, C.B., and Wang, Y.I. (2000). Mammalian spindle orientation and position respond to changes in cell shape in a dynein-dependent fashion. Mol. Biol. Cell *11*, 1765–1774.

Rodionov, V., Nadezhdina, E., and Borisy, G. (1999). Centrosomal control of microtubule dynamics. Proc. Natl. Acad. Sci. USA *96*, 115–120.

Rose, G.G., Pomerat, C.M., Shindler, T.O., and Trunnel, J.B. (1958). A cellophane strip technique for culturing tissue in multipurpose culture chambers. J. Biophys. Biochem. Cytol. *4*, 761–764.

Shaw, S.L., Yeh, E., Maddox, P., Salmon, E.D., and Bloom, K. (1997). Astral microtubule dynamics in yeast: a microtubule-based searching mechanism for spindle orientation and nuclear migration into the bud. J. Cell Biol. *139*, 985–994.

Shelden, E., and Wadsworth, P. (1993). Observation and quantification of individual microtubule behavior in vivo: microtubule dynamics are cell-type specific. J. Cell Biol. *120*, 935–945.

Straight, A.F., Marshall, W.F., Sedat, J.W., and Murray, A.W. (1997). Mitosis in living budding yeast: anaphase A but no metaphase plate. Science *277*, 574–578.

Tirnauer, J.S., and Bierer, B.E. (2000). EB1 proteins regulate microtubule dynamics, cell polarity, and chromosome stability. J. Cell Biol. *149*, 761–766.

Tirnauer, J.S., O'Toole, E., Berrueta, L., Bierer, B.E., and Pellman, D. (1999). Yeast Bim1p promotes the G1-specific dynamics of microtubules. J. Cell Biol. *145*, 993–1007.

Tournebize, R., Popov, A., Kinoshita, K., Ashford, A.J., Rybina, S., Pozniakovsky, A., Mayer, T.U., Walzak, C.E., Karsenti, E., and Hyman, A.A. (2000). Control of microtubule dynamics by the antagonistic activities of XMAP215 and XKCM1 in *Xenopus* egg extracts. Nat. Cell Biol. *2,* 13–19.

Verde, F., Dogterom, M., Stelzer, E., Karsenti, E., and Leibler, S. (1992). Control of microtubule dynamics and length by cyclin A-and cyclin B- dependent kinases in *Xenopus* egg extracts. J. Cell Biol. *118,* 1097–1108.

Vorobjev, I.A., Rodionov, V.I., Maly, I.V., and Borisy, G.G. (1999). Contribution of plus and minus end pathways to microtubule turnover. J. Cell Sci. *112*, 2277–2289.

Vorobjev, I.A., Svitkina, T.M., and Borisy, G.G. (1997). Cytoplasmic assembly of microtubules in cultured. cells. J. Cell Sci. *110*, 2635–2645.

Wadsworth, P. (1998). Microinjection of mitotic cells. Methods Cell Biol. *61*, 219–231.

Wadsworth, P. (1999). Regional regulation of microtubule dynamics in polarized, motile cells. Cell Motil. Cytoskeleton *42*, 48–59.

Waterman-Storer, C., Duey, D.Y., Weber, K.L., Keech, J., Cheney, R.E., Salmon, E.D., and Bement, W.M. (2000). Microtubules remodel actomyosin networks in *Xenopus* egg extracts via two mechanisms of F-actin transport. J. Cell Biol. *150,* 361–376.

Waterman-Storer, C.M., and Salmon, E.D. (1997). Actomyosin-based retrograde flow of microtubules in the lamella of migrating epithelial cells influences microtubule dynamic instability, induces microtubule breakage and generates non-centrosomal microtubules. J. Cell Biol. *139*, 417–434.

Yen, T.J., Machlin, P.S., and Cleveland, D.W. (1988). Autoregulated instability of β tubulin mRNAs by recognition of the nascent amino terminus of β tubulin. Nature *334*, 580–586.

Yvon, A.C., and Wadsworth, P. (1997). Non-centrosomal microtubule formation and measurement of minus end microtubule dynamics in A498 cells. J. Cell Sci. *110*, 2391–2401.